


LETTER

Clockwise and counterclockwise hysteresis characterize state changes in the same aquatic ecosystem

---

Amanda C. Northrop,<sup>1\*</sup>   
Vanessa Avalone,<sup>1</sup> Aaron M.  
Ellison,<sup>2</sup> Bryan A. Ballif<sup>1</sup> and  
Nicholas J. Gotelli<sup>1</sup>

<sup>1</sup>Department of Biology, University  
of Vermont, Burlington, VT, USA

<sup>2</sup>

---

characterizes both photosynthetic “green” food webs that experience direct nutrient enrichment and tightly linked “brown” food webs enriched with organic matter from the decomposition of primary-producer biomass (Zou et al., 2016).

Our experiments revealed that differences in the nutrient enrichment rate can generate a surprisingly rich array of recovery dynamics in the same aquatic ecosystem.

## MATERIAL AND METHODS

### The *Sarracenia* microecosystem

*Sarracenia purpurea* occurs in peat bogs and sand plains of the eastern U.S. from northern Florida to Canada, and west to the Canadian Rockies (Ellison and Gotelli, 2021). Within this large geographic range, the rain-filled leaves of the plant support an aquatic food web that rapidly assembles, consisting of a prey detrital base, shredding and filter-feeding aquatic

arthropods, and a diverse array of protozoa and microbes. The drowned prey initially are shredded by aquatic larvae of sarcophagid flies and midges, but the complete breakdown and mineralization of the prey is predominantly the result of microbial activity (Butler et al., 2008). The mineralized nutrients are quickly assimilated and translocated to plant tissues (Butler et al., 2008). In the field, less than 1% of prey encounters result in successful capture (Heard, 1998; Newell and Nastase, 1998). With low detrital inputs and active photosynthesis by the plant, this aquatic microecosystem is normally in an oligotrophic state, with low prey abundance and dissolved oxygen (DO) close to 20% (where 21% = 100% air saturation). But with excessive loading of prey or detritus, DO collapses within 8 h to less than 5% (Sirota et al., 2013). With no additional detrital enrichment, the system persists in this



(Bradford, 1976). Using sterile pipette tips, a 300  $\mu$ L aliquot was taken from 2.5 cm below the surface of each pitcher and placed in a sterile 1-mL microfuge tube. Sample tubes were immediately transported to the laboratory where they were centrifuged at 13 000g for two minutes. The supernatant containing soluble BSA was removed, placed in a sterile 1-mL microfuge tube and stored at 80  $^{\circ}$ C until analyzed.

#### BSA loading validation via SDS-PAGE

To validate that the majority of protein in extracted pitcher fluid was BSA, we ran a time series of pitcher fluid from two replicates each of the high- and low-concentration loading treatments on gels using SDS-PAGE next to known concentrations of BSA (0.1, 0.5 and 5.0 mg/ml) and a BenchMark Pre-stained Protein Ladder (Invitrogen). Ten  $\mu$ L aliquots of pitcher fluid from days 0, 2, 4, 6, 9, 12, 15, 18, 21, 24, 27 and 30 were added to 90  $\mu$ L of bromophenol blue sample buffer (150 mM Tris pH 6.8, 2% SDS, 5% beta-mercaptoethanol, 7.8% glycerol) and boiled at 95  $^{\circ}$ C for five minutes. After centrifugation at 13 000 g for 30 s, 10  $\mu$ L of each sample was mixed with 10  $\mu$ L of sample buffer and loaded into separate lanes of a 10% polyacrylamide gel (37.5:1 acrylamide:bis-

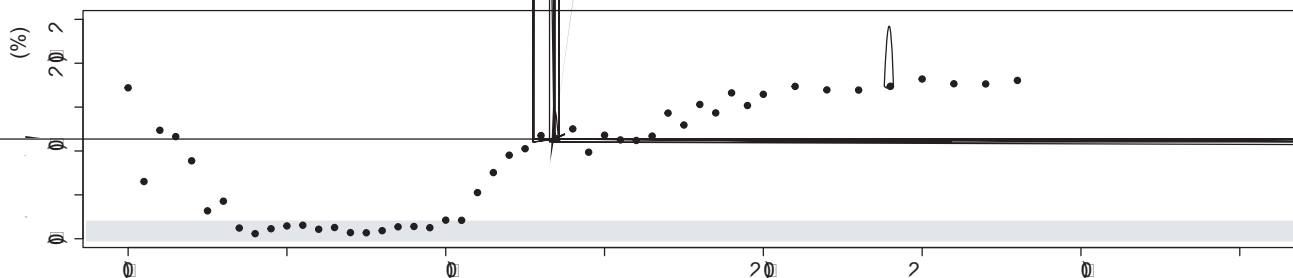
acrylamide). Gels were subjected to SDS-PAGE and stained with Coomassie.

#### Bradford assay

We used a Bradford assay (Bradford, 1976) to determine the concentration of BSA. Bradford assays were done using diluted samples after generating a standard curve with known amounts of BSA. Absorbance was measured using a Biophotometer Plus (Eppendorf) at an optical density of 600 nm. To streamline 2016 BSA concentration data collection, assays were conducted on a 96-well plate. Absorbance was measured at 545 nm with a Synergy HTX (Biotek).

#### Data analysis

We used R software (version 3.4.3) running within RStudio (v1.1.442, RStudio, Boston, MA, USA) to plot and analyze the data. We plotted the hysteresis loops using the loess function to fit curves (span= 0.75) and 95% confidence intervals to each of the interpolated enrichment and recovery trajectories. For this study, we described loop directions as "counterclockwise" and "clockwise" based on a response variable that





BSA remaining in pitchers after the cessation of enrichment that persisted for weeks (Fig. S5).

$HI_{MEAN}$  was significantly different between all enrichment treatments (ANOVA,  $F_{2,16} = 35.26$ ,  $P < 0.001$ ). Moreover the hysteresis index differed significantly between each of the three unique pairs of treatments (Tukey's HSD,  $P < 0.001$ ). Pitchers receiving a low rate of BSA enrichment displayed a clockwise hysteresis loop in the relationship between BSA concentration and DO, with a lag in DO recovery relative to decreasing BSA concentration during the recovery phase ( $HI_{MEAN} = -0.247$ ; Figs 3 and 4, Figs S3 and S6). Hysteresis was absent at intermediate levels of enrichment: enrichment and recovery curves overlapped, suggesting a responsive tracking of BSA concentration by DO ( $HI_{MEAN} = -0.014$ ; Figs 3 and 4, Figs S3, and S6). High levels of BSA enrichment yielded a counterclockwise hysteresis loop: DO changed faster per unit change in BSA concentration during recovery than enrichment ( $HI_{MEAN} = 0.210$ ; Figs 3 and 4, Figs S3 and S6).

## DISCUSSION

We have shown that an enriched aquatic ecosystem can display a diverse set of hysteretic responses modulated by changes in a single driver variable. At low levels of enrichment, there was a strong clockwise hysteresis loop in which recovery of oxygen lags behind changes in BSA. In contrast, high levels of enrichment yielded a counter-clockwise loop. Counter-clockwise hysteresis has been detected in some physical and biological (Grigg and Seebacher, 1999; Huet al.,

2012; Louizos et al., 2014) systems, but has rarely been documented in ecological studies. The few ecological studies with counterclockwise hysteresis loops quantify static patterns of hydrological relationships along a spatial gradient, rather than measuring ecosystem dynamics and changes through time (Whitfield and Schreier, 1981; Huang et al., 2017).

It is worth noting that  $HI_{MEAN}$  describes hysteresis as a single number for each replicate ecosystem, but does not characterize variation among time points within a replicate. In the low enrichment treatment, confidence intervals for the loess fit are nearly overlapping; however, both high and low enrichment treatments differ in sign but have  $HI_{MEAN}$  values of similar magnitude. When all replicates are normalized and pooled within treatments (Fig. S7), a single  $HI_{MEAN}$  for each treatment still exhibits the same rank order as in the analysis with proper ecosystem replication: low < intermediate < high ( $-0.021 < 0.063 < 0.184$ ).

An analytical systems model of the *S. purpurea* ecosystem predicts clockwise hysteresis as a result of smooth changes in photosynthesis coupled with an abrupt increase in biological oxygen demand (BOD) (Lau et al., 2018). Indeed, the addition

In other systems, counter-clockwise hysteresis is generally the result of positive feedback loops (Korbel et al., 2016). In our system, positive relationships exist between plant photosynthesis and DO, bacterial abundance and BSA, and potentially between the abundance of facultatively anaerobic bacteria and DO. A minimal model of the system would include such variables as the abundance of aerobic and anaerobic bacteria and the concentration of DO and BSA.

The magnitude of hysteresis is influenced by changes in the strength of feedbacks underlying the hysteresis response (Garnier et al., 2019). We hypothesize that the changes in magnitude and direction of hysteresis in our system are a result of changing feedback strengths between bacterial abundance, DO and BSA concentration. Although we did not measure bacterial abundance, we suspect there were dramatic increases because pitcher fluid in enriched pitchers was cloudy and brown after enrichment. Complex hysteretic dynamics may also reflect changes in microbial composition and function; indeed, ongoing proteomic assays reveal increases in protein expression in facultative anaerobes as a result of BSA loading (in prep).

Hysteretic ecosystems may require larger restoration efforts to recover from a regime shift (Mayer and Reitkerk, 2004). For example, in eutrophic shallow lakes, a simple reduction in phosphorus input does not lead to a proportional recovery in macrophyte cover (Meijer, 2000) or community structure (Sand-Jensen et al., 2016). Furthermore, these communities do not fully recover in the time frames in which they are studied (Sand-Jensen et al., 2016) and may effectively remain permanently degraded. These examples and our work highlight the importance of applying a dynamic regime concept (Mayer and Reitkerk, 2004) to ecosystem management and restoration. Such an approach would include testing for hysteresis, characterizing feedbacks that maintain undesirable regimes, and identifying if and how variables change as a result of d

regime shift (udging

In ecosystems, counter-clockwise hysteresis is characterized by a reduction in variables that is not reversible.

When a system is subjected to a disturbance, it may undergo a regime shift (Mayer and Reitkerk, 2004). In ecosystems, counter-clockwise hysteresis is characterized by a reduction in variables that is not reversible.

When a system is subjected to a disturbance, it may undergo a regime shift (Mayer and Reitkerk, 2004). In ecosystems, counter-clockwise hysteresis is characterized by a reduction in variables that is not reversible.

When a system is subjected to a disturbance, it may undergo a regime shift (Mayer and Reitkerk, 2004). In ecosystems, counter-clockwise hysteresis is characterized by a reduction in variables that is not reversible.

to restore

highlights work

enrichment

hys

